

# Functional MRI with Magnetization Transfer Effects: Determination of BOLD and Arterial Blood Volume Changes

Tae Kim,<sup>1\*</sup> Kristy Hendrich,<sup>1</sup> and Seong-Gi Kim<sup>1,2</sup>

The primarily intravascular magnetization transfer (MT)-independent changes in functional MRI (fMRI) can be separated from MT-dependent changes. This intravascular component is dominated by an arterial blood volume change ( $\Delta\text{CBV}_a$ ) term whenever venous contributions are minimized. Stimulation-induced  $\Delta\text{CBV}_a$  can therefore be measured by a fit of signal changes to MT ratio. MT-varied fMRI data were acquired in 13 isoflurane-anesthetized rats during forepaw stimulation at 9.4T to simultaneously measure blood-oxygenation-level-dependent (BOLD) and  $\Delta\text{CBV}_a$  response in somatosensory cortical regions. Transverse relaxation rate change ( $\Delta R_2$ ) without MT was  $-0.43 \pm 0.15 \text{ s}^{-1}$ , and MT ratio decreased during stimulation.  $\Delta\text{CBV}_a$  was  $0.46 \pm 0.15 \text{ ml}/100 \text{ g}$ , which agrees with our previously-presented MT-varied arterial-spin-labeled data ( $0.42 \pm 0.18 \text{ ml}/100 \text{ g}$ ) in the same animals and also correlates with  $\Delta R_2$  without MT. Simulations show that  $\Delta\text{CBV}_a$  quantification errors due to potential venous contributions are small for our conditions. *Magn Reson Med* 60: 1518–1523, 2008. © 2008 Wiley-Liss, Inc.

**Key words:** magnetization transfer; fMRI; BOLD; arterial blood volume; high magnetic field

Off-resonance RF pulses can significantly reduce extravascular signals by magnetization transfer (MT) from tissue macromolecule protons to tissue water protons, while intravascular (arterial and venous) signals are much less affected due to low macromolecule concentration in blood (1,2). Signal intensity measurements with vs. without off-resonance irradiation give the MT attenuation factor ( $1 - \text{MTR}$ ), where MTR is the MT ratio, which accounts for both MT (spin exchange and cross relaxation) and any potential direct saturation effects of the off-resonance pulse (3). Functional blood-oxygenation-level-dependent (BOLD) studies incorporating off-resonance spin preparation have examined the effects on functional MRI (fMRI) contrast (4–6). Initially, human neural activation studies found that MT reduced the BOLD percentage signal change for most activated pixels, and that MTR increased with task activation (5). In contrast, recent hypercapnia studies in rat found that MT increased the BOLD percentage signal change, and that MTR decreased with arterial

partial pressure of  $\text{CO}_2$  ( $\text{PACO}_2$ ) levels (6). Further studies are necessary to understand BOLD signals with MT effects.

Properties of MT-dependent extravascular (tissue) signals and mostly MT-insensitive intravascular (blood) signals can be utilized to enhance arterial and venous contributions to BOLD signal changes. Venous contributions are minimal when capillary water freely exchanges with tissue water, or when the echo time (TE) is long relative to venous blood  $T_2$  (7), leaving terms involving the arterial blood volume change ( $\Delta\text{CBV}_a$ ) as the dominant MT-independent contribution to stimulus-induced changes. A similar concept was applied in the previously-described MT-varied fMRI experiments in our companion article using arterial spin labeling (ASL) (8). For this work, we utilize these pool-dependent MT properties without ASL to investigate the effects on BOLD fMRI contrast and quantify  $\Delta\text{CBV}_a$  from MT-varied BOLD 9.4T data on rat somatosensory cortex. Individual  $\Delta\text{CBV}_a$  values from MT-varied BOLD data are compared with  $\Delta\text{CBV}_a$  values from our previously-reported MT-varied ASL data (8), and with transverse relaxation rate changes ( $\Delta R_2$ ). Errors in  $\Delta\text{CBV}_a$  quantification due to potential venous contributions were simulated.

## THEORY

It is assumed that an imaging voxel consists of three compartments; intravascular arterial blood, extravascular tissue, and intravascular venous blood. Capillaries are included in the tissue compartment when capillary water freely exchanges with tissue water, while any unexchanged portion is split between arterial and venous compartments. Studies of *stationary* blood phantoms determined that blood MTR/tissue MTR  $\approx 0.4$  (9,10). But when *flowing* blood spins replace those affected by MT (as for certain RF coil geometries), arterial pool MT effects are minimized (8). If the spin-preparation period is long relative to the water exchange time of  $\approx 500 \text{ ms}$ , (11), capillary water will freely exchange with tissue water, and this upstream exchange could create significant MT effects in venous blood. With complete exchange, venous MTR = tissue MTR; otherwise, venous MTR will depend on MT pulse exposure time.

Steady-state spin-echo (SE) signal intensity from all compartments in the presence of MT ( $S_{MT}$ ) can be expressed as

$$S_{MT} = v_a \cdot M_0 \cdot \exp(-R_{2,a} \cdot TE) + (1 - v_a - v_v) \cdot (1 - \text{MTR}) \cdot M_0 \cdot \exp(-R_{2,t} \cdot TE) + v_v \cdot (1 - \kappa \cdot \text{MTR}) \cdot M_0 \cdot \exp(-R_{2,v} \cdot TE), \quad [1]$$

<sup>1</sup>Department of Radiology, University of Pittsburgh, Pittsburgh, Pennsylvania, USA.

<sup>2</sup>Department of Neurobiology, University of Pittsburgh, Pittsburgh, Pennsylvania, USA.

Grant sponsor: National Institutes of Health (NIH); Grant numbers: EB003375, EB003324, NS44589, RR17239.

\*Correspondence to: Tae Kim, Ph.D., Department of Radiology, University of Pittsburgh Medical School, 3025 East Carson Street, Pittsburgh, PA 15203. E-mail: tak19@pitt.edu

Received 22 February 2008; revised 29 May 2008; accepted 7 July 2008.

DOI 10.1002/mrm.21766

Published online in Wiley InterScience (www.interscience.wiley.com).

© 2008 Wiley-Liss, Inc.

where subscripts  $a$ ,  $t$ , and  $v$  represent intravascular arterial, extravascular tissue, and intravascular venous compartments, respectively;  $\nu$  is the fraction of spins in each blood pool (% units);  $R_2$  is the transverse relaxation rate;  $MTR \approx$  tissue MTR, calculated as  $(1 - S_{MT}/S_0)$ , where  $S_0$  is baseline signal intensity without MT, and  $\kappa$  = venous blood MTR/tissue MTR. Gradient-echo implementation would require substitution of effective transverse relaxation rates ( $R_{2}^*$  for arterial tissue and venous blood compartments in Eq. [1]).

During neural stimulation, it is reasonable to assume that  $R_{2,a}$  does not change. Signal intensity during stimulation ( $S_{stim,MT}$ ) accounting for potential changes in  $R_{2,t}$  and  $R_{2,v}$  ( $\Delta R_{2,t}$  and  $\Delta R_{2,v}$ ), changes in arterial and venous blood volumes ( $\Delta v_a$  and  $\Delta v_v$ ) and a decrease in tissue volume is then

$$S_{stim,MT} = (v_a + \Delta v_a) \cdot M_0 \cdot \exp(-R_{2,a} \cdot TE) + (1 - v_a - v_v - \Delta v_a - \Delta v_v) \cdot (1 - MTR) \cdot M_0 \cdot \exp[-(R_{2,t} + \Delta R_{2,t}) \cdot TE] + (v_v + \Delta v_v) \cdot (1 - \kappa \cdot MTR) \cdot M_0 \cdot \exp[-(R_{2,v} + \Delta R_{2,v}) \cdot TE]. \quad [2]$$

Under assumptions that arterial and venous blood contributions to baseline are very small (i.e.,  $S_0 \approx M_0 \exp(-R_{2,t} \cdot TE)$ ), and that both  $\Delta R_{2,t} \cdot TE$  and  $\Delta R_{2,v} \cdot TE$  are very small, the stimulation-induced signal change in the presence of MT ( $\Delta S_{stim,MT} = S_{stim,MT} - S_{MT}$ ) normalized to  $S_0$  becomes

$$\Delta S_{stim,MT}/S_0 \approx \Delta v_a \cdot \exp[-(R_{2,a} - R_{2,t}) \cdot TE] + [(1 - v_a - v_v - \Delta v_a - \Delta v_v) \cdot (-\Delta R_{2,t} \cdot TE) - (\Delta v_a + \Delta v_v) \cdot (1 - MTR) + (v_v + \Delta v_v) \cdot (-\Delta R_{2,v} \cdot TE) + \Delta v_v \cdot (1 - \kappa \cdot MTR) \cdot \exp[-(R_{2,v} - R_{2,t}) \cdot TE]. \quad [3]$$

Equation [3] can be simplified for either of the following conditions: 1) If capillary and tissue water freely exchange ( $\kappa = 1$ ), venous MTR = tissue MTR, and both tissue (second) and venous (last) terms can then be combined into a single term with a factor ( $A$ ) multiplied by  $(1 - MTR)$ . 2) Even for  $\kappa \neq 0$ , the venous (third) term is minimized whenever TE is appropriately long relative to venous blood  $T_2$ —a condition easily satisfied at 9.4T where  $R_{2,v} \approx 150$  to  $200 \text{ s}^{-1}$  (7,12). Under either of these conditions,

$$\Delta S_{stim,MT}/S_0 \approx \Delta v_a \cdot \exp[-(R_{2,a} - R_{2,t}) \cdot TE] + A \cdot (1 - MTR). \quad [4]$$

At 9.4T, the arterial term is approximately  $\Delta v_a$ , since  $R_2$  values of arterial blood and tissue are similar ( $R_{2,a} \approx R_{2,t} \approx 25 \text{ s}^{-1}$  (7)), leaving

$$\Delta S_{stim,MT}/S_0 \approx \Delta v_a + A \cdot (1 - MTR), \quad [5]$$

so that for a linear fit of  $\Delta S_{stim,MT}/S_0$  vs.  $(1 - MTR)$ , the intercept yields  $\Delta v_a$ , which is converted to  $\Delta CBV_a$  (units of ml/g tissue) by multiplying by the tissue-to-blood partition coefficient of 0.9 ml/g (13).

Conventional fMRI responses have volume and relaxation components from arteries, tissue and veins. Pure BOLD responses (i.e., with origins in tissue and veins) can be obtained by removal of terms directly related to  $\Delta v_a$  under conditions where  $\Delta v_v$  is minimal (8); this is accomplished by subtracting  $\Delta v_a \cdot (\exp[-(R_{2,a} - R_{2,t}) \cdot TE] - 1)$  from fMRI signal change without MT (see Eq. [3] with  $MTR = 0$ ). At 9.4T, this correction is unnecessary since  $R_{2,a} = R_{2,t}$ .

## MATERIALS AND METHODS

### Animal Preparation

Animal protocol was approved by the University of Pittsburgh Animal Care and Use Committee. Thirteen male Sprague-Dawley rats weighing 350–450 g (Charles River Laboratories, Wilmington, MA, USA) were studied under 1.3% to 1.5% isoflurane anesthesia. Details of animal preparation were described previously (8). Animals were maintained within normal physiological ranges; pressure of  $\text{CO}_2$  ( $\text{PaCO}_2$ ) =  $38.1 \pm 4.6$  mmHg,  $\text{PaO}_2$  =  $110.2 \pm 11.6$  mmHg, and mean arterial blood pressure =  $93.1 \pm 8.01$  mmHg ( $N = 13$ ). Forepaw stimulation parameters were pulse duration = 3 ms, pulse current = 1.5–1.8 mA, pulse frequency = 6 Hz (14), stimulus duration = 15 s, and interstimulus period >1 min. No significant blood pressure changes were observed during somatosensory stimulation.

### MRI Methods

Images were acquired at 9.4T (magnet bore size = 31-cm diameter), with a Unity INOVA console (Varian, Palo Alto, CA, USA). A 2.3-cm diameter surface coil on the head provided for variable MT effects and image acquisition capability; arterial MT effects were negligible due to the flow of arterial blood into the limited region of imaging coil coverage (8). A butterfly-shaped surface coil over the neck provided the arterial-spin labeling required only for our previously-presented data (8). Both RF coils were actively detunable. There is no possibility for interference between spin labeling and MT effects with this coil configuration. Magnetic field homogeneity was manually optimized on a slab double the imaging slice thickness. Data acquisition used an adiabatic version of the single-shot SE echo-planar imaging (EPI) technique with coronal slice thickness = 2 mm, matrix size = 64 (readout)  $\times$  32 (phase-encode), field of view =  $3.0 \times 1.5 \text{ cm}^2$ , repetition time = 2.5 s, and TE = 40 ms ( $N = 7$ ) or 30 ms ( $N = 6$ ).

Target MTR values were 0, 0.3, and 0.5 for gray matter (corresponding  $B_1$  field strengths were 0, 0.11, and 0.16 Gauss, respectively). The head surface coil transmitted MT pulses at +8500 Hz offset relative to water to guarantee irradiation of macromolecular protons, without direct saturation of any water protons (6). The 2.4-s spin-preparation period contained twelve 100-ms MT pulses separated by 100-ms intervals, during which spin-tagging pulses were applied both for labeled and unlabeled data, but only unlabeled data were used for MT-varied BOLD studies. Sixteen pairs of arterial-spin labeled and unlabeled images (in alternating order) were acquired for each MT level with

five prestimulation control pairs, three stimulation pairs, and eight poststimulus pairs. Although the MT-induced signal may not reach steady-state during a single 2.4-s spin-preparation period, the 0.1-s acquisition time allowed virtually-continuous spin preparation during fMRI studies, ensuring steady-state MT conditions. Other experimental details appear in our previous report on MT-varied ASL measurement of  $\Delta\text{CBV}_a$  during somatosensory stimulation (8), where  $\Delta\text{CBF}$  and  $\Delta\text{CBV}_a$  were obtained from both arterial-spin labeled and unlabeled images. In this work, BOLD and  $\Delta\text{CBV}_a$  responses were determined solely from unlabeled images with varied MT.  $\Delta\text{CBV}_a$  values computed by both approaches were compared.

### Data Processing

For each animal, *all* runs from identical conditions were averaged, where the baseline condition included all pre-stimulation data, and the stimulation condition included data acquired between 5 and 15 s after stimulation onset. Data were subsequently processed as previously described for  $\Delta\text{CBV}_a$  quantification with MT-varied ASL (8) except that only unlabeled images were used. Since a rat brain atlas (15) shows a forelimb somatosensory cortical area of  $\sim 1.5 \times 1.5 \text{ mm}^2$  in coronal plates 0.2 and 0.3 mm anterior to bregma, a 9-pixel region of interest (ROI) ( $1.4 \times 1.4 \text{ mm}^2$ ) centered over this anatomically-defined area on the side contralateral to stimulation was defined for all quantifications in each animal. The presence of MT-independent contributions to BOLD fMRI was initially assessed by plotting  $-\Delta R_2$  values [ $= (\Delta S_{stim,MT}/S_{MT})/TE$ ] vs. MTR calculated from baseline data. Normalized functional signal changes ( $\Delta S_{stim,MT}/S_0$ ) were linearly fitted against

normalized signals from baseline conditions ( $S_{MT}/S_0 = 1 - \text{MTR}$ ), and  $\Delta\text{CBV}_a$  was calculated from the intercept in each study. These  $\Delta\text{CBV}_a$  values for individual animals were compared with companion report values (8) for the same ROI obtained by MT-varied ASL. Individual results were averaged and group data are reported as mean  $\pm$  SD. Statistical analyses were performed using paired *t*-tests (Origin 7.0, Northampton, MA, USA). Maps of  $\Delta S_{stim,MT}/S_{MT}$  were generated for active pixels with *P*-values  $< 0.05$  for illustrative purposes only.

### Simulations of $\Delta\text{CBV}_a$ Quantification Errors

If assumptions for our conditions about negligible venous-term contributions in Eq. [3] are incorrect, then Eq. [5] may be oversimplified. Errors in our  $\Delta\text{CBV}_a$  values were therefore assessed using Eq. [3] for the following conditions: at baseline  $v_a = 0.9\%$  and  $v_a + v_v = 3.5\%$ ; venous oxygenation level ( $Y$ ) = 0.6 or 0.7 (8);  $R_{2,a} = R_{2,t} = 25 \text{ s}^{-1}$  and  $R_{2,v} = 478 - (458 \cdot Y) \text{ s}^{-1}$  (7);  $\Delta R_{2,t} \approx \Delta R_2 = -0.43 \text{ s}^{-1}$ ,  $\Delta R_{2,v} = -458 \cdot \Delta Y \text{ s}^{-1}$  (derived from Ref. 7); and  $TE = 35 \text{ ms}$ . Since  $\Delta v_v$  is minimal for our conditions (8), we assess errors in  $\Delta\text{CBV}_a$  quantification with  $\Delta v_v = 0\%$ , as a function of  $\kappa$  values and stimulus-induced changes in  $Y$  ( $\Delta Y$ ) = 0.04, 0.06, 0.08, and 0.1.

## RESULTS

Baseline EPI signals ( $S_{MT}$ ) decreased with *MTR* as expected, as demonstrated in the grayscale image from one animal (Fig. 1a). Substantial functional changes ( $\Delta S_{stim,MT}/S_{MT}$ ) observed for all *MTR* values increased with *MTR* in the somatosensory ROI (color maps, Fig. 1a). Individual

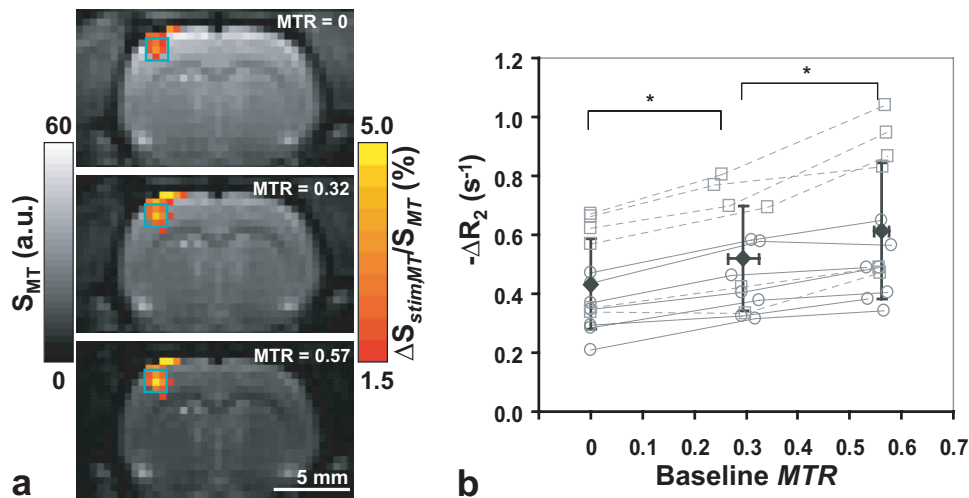


FIG. 1. MT-varied BOLD fMRI responses to somatosensory stimulation. **a**: Grayscale baseline EPI images from one animal are overlaid with color maps of stimulation-induced percentage change (no spatial smoothing was performed). The hemisphere contralateral to stimulation appears on the left in images. As *MTR* increases, baseline signal intensity (a.u. = arbitrary units) decreases, while percentage signal change ( $\Delta S_{stim,MT}/S_{MT}$ ) increases in the contralateral somatosensory area. Green square overlays show 9-pixel ROI in the somatosensory area. **b**: Interanimal comparisons within somatosensory ROIs show stimulus-induced changes to  $R_2$  [ $-\Delta R_2 = (\Delta S_{stim,MT}/S_{MT})/TE$ ] vs. *MTR* calculated from the baseline data. The statistically-significant change in  $\Delta R_2$  between target *MTR* values ( $*P < 0.01$ ,  $N = 13$ ) reflects the increasing intravascular contribution to  $\Delta R_2$  with *MTR*. Open symbols show individual animal's data at each *MTR* value for  $TE = 30 \text{ ms}$  (squares connected with dashed lines) or  $TE = 40 \text{ ms}$  (circles connected with solid lines), while filled diamonds show mean data, where error bars are SD.

subject's  $-\Delta R_2$  values within somatosensory ROIs plotted against  $MTR$  values calculated from prestimulus data show that mean BOLD signal changes also increased with  $MTR$  (Fig. 1b), with  $\Delta R_2 = -0.43 \pm 0.15, -0.52 \pm 0.17,$  and  $-0.61 \pm 0.23 \text{ s}^{-1}$  at baseline  $MTR = 0, 0.294 \pm 0.030$  and  $0.561 \pm 0.013,$  respectively ( $N = 13$ ). Corresponding stimulation-condition  $MTR$  values =  $0, 0.292 \pm 0.029$  and  $0.558 \pm 0.013$  ( $N = 13$ ); although these stimulation vs. baseline  $MTR$  decreases are small relative to SD, the decreases were seen for each animal and are statistically significant ( $P < 0.01$ ).

Neural activity-induced  $\Delta CBV_a$  was determined from a linear fit of  $\Delta S_{stim,MT}/S_0$  vs.  $S_{MT}/S_0$  ( $= 1 - \text{baseline } MTR$ ) (Fig. 2). The intercept yields  $v_a = 0.51 \pm 0.17 \%$  ( $N = 13$ ), which converts to  $\Delta CBV_a = 0.46 \pm 0.15 \text{ ml}/100 \text{ g}$ . Individual animal's BOLD signal changes ( $-\Delta R_2$  values without MT) vs.  $\Delta CBV_a$  values are well correlated (Fig. 3,  $R^2 = 0.49$ ). Comparison of  $\Delta CBV_a$  determined for individual animals with the MT-varied BOLD approach vs. the MT-varied ASL approach (Fig. 4) shows a good correlation with no statistical differences ( $R^2 = 0.72, P = 0.15$ ).

In the absence of free exchange, quantification of our MT-varied BOLD data accounting for non-negligible venous-term contributions yields  $\Delta CBV_a$  values that are reduced as  $Y$  increases,  $\Delta Y$  increases, or venous/tissue MT effects ( $\kappa$ ) are reduced (Fig. 5). For reasonable  $\kappa$  values ( $>0.4$ ), the maximum overestimation of  $\Delta CBV_a$  is  $0.06 \text{ ml}/100 \text{ g}$  for  $0.46 \text{ ml}/100 \text{ g}$ .

**DISCUSSION**

Our MT-varied BOLD rat forepaw stimulation studies at 9.4T show enhanced signal changes due to MT-insensitive

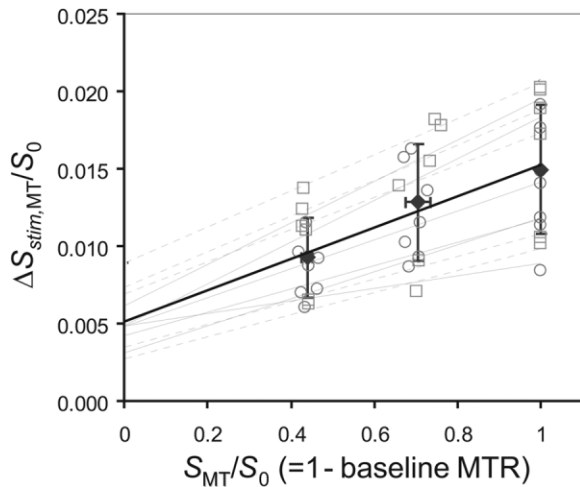


FIG. 2. Normalized stimulus-induced BOLD fMRI changes ( $\Delta S_{stim,MT}/S_0$ ) vs. baseline MT attenuation factor within somatosensory ROIs ( $N = 13$ ). A linear fit to all data (thick solid line) yields  $\Delta S_{stim,MT}/S_0 = 0.0101 \cdot (1 - MTR) + 0.0051, R^2 = 0.9708$ . The 0.51% intercept represents the MT-independent change for the fraction of spins in the arterial blood pool due to neural activation, and corresponds to a  $\Delta CBV_a$  value of  $0.46 \text{ ml}/100 \text{ g}$ . Open symbols show individual animal's data at each  $MTR$  value for TE = 30 ms (squares connected with gray dashed lines) or TE = 40 ms (circles connected with gray solid lines), while filled diamonds show mean data, where error bars are SD.

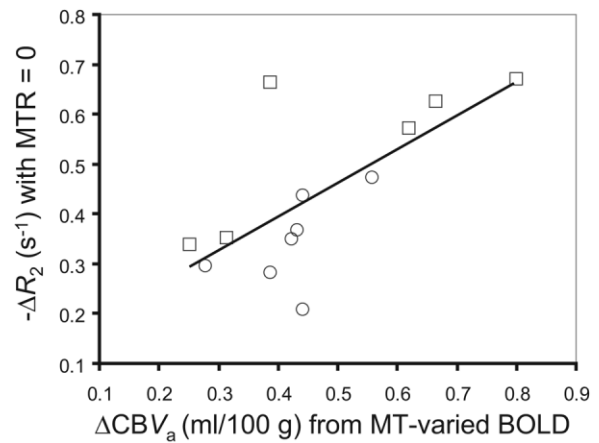


FIG. 3. Conventional BOLD signal changes ( $-\Delta R_2$  without MT) vs.  $\Delta CBV_a$  calculated from MT-varied BOLD within somatosensory ROIs ( $N = 13$ ). Measured  $\Delta CBV_a$  is well correlated with BOLD; line shows fit to  $-\Delta R_2 = 0.68 \cdot \Delta CBV_a + 0.12$  ( $R^2 = 0.49$ ). Individual animal's data for TE = 30 ms (squares) or TE = 40 ms (circles).

intravascular contributions. Under the conditions of the present 9.4T MT-varied BOLD study, venous-term contributions to the MT-independent signal should be minimal, leaving primarily  $\Delta CBV_a$  contributions; if any venous blood contributions do exist,  $\Delta CBV_a$  is only slightly overestimated. At low magnetic field, the potential of a significant venous term in Eq. [3] means that successful  $\Delta CBV_a$  quantification depends on  $\kappa$ ; when  $\kappa \neq 1$ , our approach is not applicable, whenever  $\kappa = 1$  (independent of field), the intercept of a linear fit of  $\Delta S_{stim,MT}/S_0$  vs.  $(1 - MTR)$  from

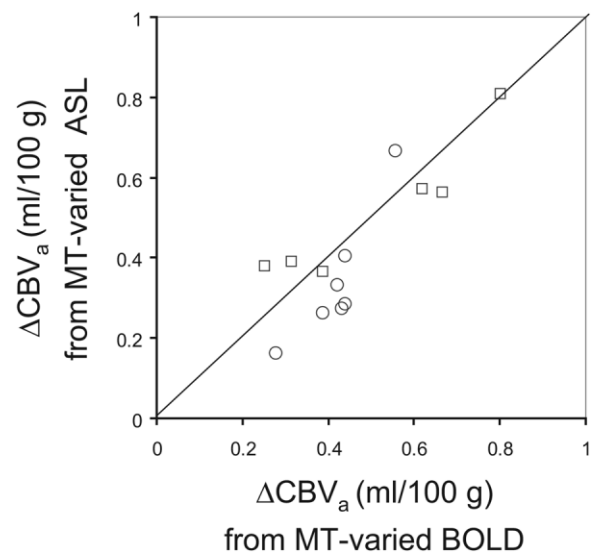


FIG. 4. Interanimal comparison of stimulus-induced  $\Delta CBV_a$  calculated from MT-varied ASL data vs. MT-varied BOLD data within somatosensory ROIs ( $N = 13$ ). A line of unity shows that  $\Delta CBV_a$  values determined for individual animals by both methods are statistically similar ( $P = 0.15, R^2 = 0.72, N = 13$ ). Open symbols show individual animal's data for TE = 30 ms (squares) and TE = 40 ms (circles).

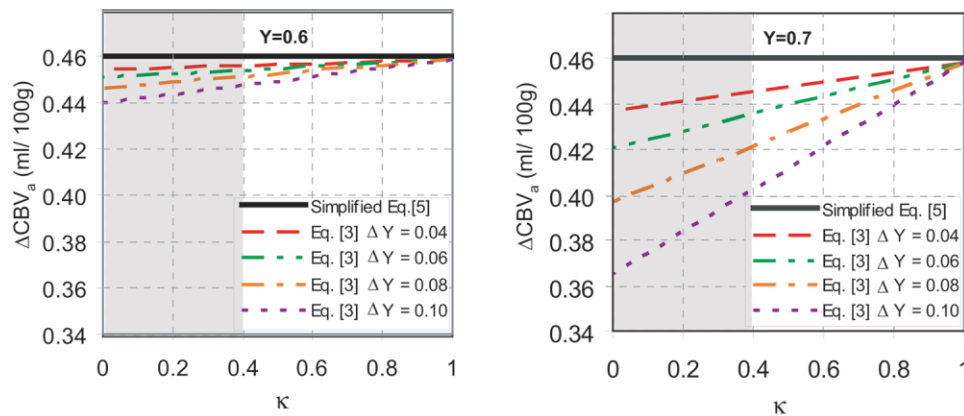


FIG. 5. Simulations show that potential  $\Delta\text{CBV}_a$  quantification errors from our MT-varied BOLD data are small using simplified Eq. [5] vs. Eq. [3] with  $\Delta v_v = 0\%$ . Eq. [3] accounts for non-negligible venous blood contributions in the absence of free exchange between capillary and tissue water; simulations are for baseline venous blood oxygenation levels ( $Y$ ) of 0.6 (a) and 0.7 (b), as a function of stimulus-induced venous oxygenation changes ( $\Delta Y$ ) and ratio of venous MTR to tissue MTR ( $\kappa$ ). Parameters appear in the “Simulations of  $\Delta\text{CBV}_a$  Quantification Errors” section of Materials and Methods. Horizontal lines in (a) and (b) represent the  $\Delta\text{CBV}_a$  value of 0.46 ml/100 g obtained with Eq. [5], which ignores the venous (third) term of Eq. [3]. A reasonable lower limit for  $\kappa$  is 0.4, based on measurements of a stationary blood phantom (9,10), and the fact of that significant exchange between blood and tissue during the MT spin-preparation period should increase  $\kappa$ ; regions that are not gray therefore indicate likely in vivo  $\kappa$  values. It should be noted that Eq. [5] is valid under the conditions of free exchange ( $\kappa = 1$ ), even with a non-negligible venous blood term in Eq. [3].

Eq. [4] can be used to quantify  $\Delta\text{CBV}_a$  if  $R_{2,a}$  and  $R_{2,t}$  are known.

Quantification of  $\Delta\text{CBV}_a$  from the same group of animals ( $N = 13$ ) with MT-varied BOLD vs. MT-varied ASL (8) are well matched ( $0.46 \pm 0.15$  ml/100 g vs.  $0.42 \pm 0.18$  ml/100 g, respectively) (Fig. 4). Our  $\Delta v_a$  values of  $0.51 \pm 0.17\%$  are considerably smaller than those of  $1.2 \pm 0.7\%$  for human finger movement at 3T recently measured with Look-Locker EPI acquisition of ASL data with multiple inversion times following one inversion pulse (16). The discrepancy may be due to differences in species, anesthesia, and/or technique-dependent measurement errors.

Our findings of BOLD signal increases with MT due to increased intravascular contributions agree with other recent studies (6), but our theory also incorporates any potential MT sensitivity within the vasculature. These findings are not consistent with one study using short TR and low MTR, where there may have been more progressive saturation in blood than in tissue (5). At 9.4T,  $T_1$  of tissue and blood (2.0 s vs. 2.3 s) are similar (17), minimizing any progressive saturation differences. A spectroscopic finding of decreased MTR with neuronal depolarization was attributed to relaxation time changes, as opposed to any change in the true MT effect (18). However, under our normal physiological conditions, any relaxation time changes due to neural activation are likely to be very small.

Our method to measure  $\Delta\text{CBV}_a$  from MT-varied BOLD fMRI is a simple technique implementable with a single coil of limited RF coverage that could also be used in human studies. This approach only determines  $\Delta\text{CBV}_a$ , but could provide higher temporal resolution than ASL with varied MT (17) or with bipolar gradients (19), although the latter approach provides baseline  $\text{CBV}_a$ , functional  $\Delta\text{CBV}_a$  and functional perfusion changes.

## ACKNOWLEDGMENTS

The 9.4T system was funded in part by an NIH grant (RR17239).

## REFERENCES

1. Wolff SD, Balaban RS. Magnetization transfer contrast (MTC) and tissue water proton relaxation in vivo. *Magn Reson Med* 1989;10:135–144.
2. Balaban RS, Chesnick S, Hedges K, Samaha F, Heineman FW. Magnetization transfer contrast in MR imaging of the heart. *Radiology* 1991; 180:671–675.
3. Henkelman RM, Huang X, Xiang QS, Stanisz GJ, Swanson SD, Bronskill MJ. Quantitative interpretation of magnetization transfer. *Magn Reson Med* 1993;29:759–766.
4. Song AW, Wolff SD, Balaban RS, Jezzard P. The effect of off-resonance radiofrequency pulse saturation on fMRI contrast. *NMR Biomed* 1997; 10:208–215.
5. Zhang R, Cox RW, Hyde JS. The effect of magnetization transfer on functional MRI signals. *Magn Reson Med* 1997;38:187–192.
6. Zhou J, Payen JF, van Zijl PC. The interaction between magnetization transfer and blood-oxygen-level-dependent effects. *Magn Reson Med* 2005;53:356–366.
7. Lee SP, Silva AC, Ugurbil K, Kim SG. Diffusion-weighted spin-echo fMRI at 9.4 T: microvascular/tissue contribution to BOLD signal changes. *Magn Reson Med* 1999;42:919–928.
8. Kim T, Hendrich KS, Masamoto K, Kim SG. Arterial versus total blood volume changes during neural activity-induced cerebral blood flow change: implication for BOLD fMRI. *J Cereb Blood Flow Metab* 2007; 27:1235–1247.
9. Niemi PT, Komu ME, Koskinen SK. Tissue specificity of low-field-strength magnetization transfer contrast imaging. *J Magn Reson Imaging* 1992;2:197–201.
10. Pike GB, Hu BS, Glover GH, Enzmann DR. Magnetization transfer time-of-flight magnetic resonance angiography. *Magn Reson Med* 1992; 25:372–379.
11. Sanders JA, Orrison WW. Functional magnetic resonance imaging. In: *Functional Brain Imaging*. St. Louis: Mosby; 1995. p 239–326.
12. Jin T, Wang P, Tasker M, Zhao F, Kim SG. Source of nonlinearity in echo-time-dependent BOLD fMRI. *Magn Reson Med* 2006;55:1281–1290.
13. Herscovitch P, Raichle ME. What is the correct value for the brain-blood partition coefficient for water? *J Cereb Blood Flow Metab* 1985; 5:65–69.

14. Masamoto K, Kim T, Fukuda M, Wang P, Kim SG. Relationship between neural, vascular, and BOLD signals in isoflurane-anesthetized rat somatosensory cortex. *Cereb Cortex* 2007;17:942–950.
15. Paxinos G, Watson C. *The rat brain in stereotaxic coordinates*. 2nd edition. San Diego: Academic Press; 1986.
16. Brookes MJ, Morris PG, Gowland PA, Francis ST. Noninvasive measurement of arterial cerebral blood volume using Look-Locker EPI and arterial spin labeling. *Magn Reson Med* 2007;58:41–54.
17. Kim T, Kim SG. Quantification of cerebral arterial blood volume and cerebral blood flow using MRI with modulation of tissue and vessel (MOTIVE) signals. *Magn Reson Med* 2005;54:333–342.
18. Stanisz GJ, Yoon RS, Joy ML, Henkelman RM. Why does MTR change with neuronal depolarization? *Magn Reson Med* 2002;47:472–475.
19. Kim T, Kim SG. Quantification of cerebral arterial blood volume using arterial spin labeling with intravoxel incoherent motion-sensitive gradients. *Magn Reson Med* 2006;55:1047–1057.